

PROCEEDINGS OF SPIE

[SPIDigitalLibrary.org/conference-proceedings-of-spie](https://spiedigitallibrary.org/conference-proceedings-of-spie)

Acoustic streaming effects in megasonic cleaning of EUV photomasks: a continuum model

Kapila, Vivek, Deymier, Pierre, Shende, Hrishikesh, Pandit, Viraj, Raghavan, Srin, et al.

Vivek Kapila, Pierre A. Deymier, Hrishikesh Shende, Viraj Pandit, Srin Raghavan, Florence Odile Eschbach, "Acoustic streaming effects in megasonic cleaning of EUV photomasks: a continuum model," Proc. SPIE 5992, 25th Annual BACUS Symposium on Photomask Technology, 59923X (8 November 2005); doi: 10.1117/12.633378

SPIE.

Event: SPIE Photomask Technology, 2005, Monterey, California, United States

Acoustic Streaming Effects in Megasonic Cleaning of EUV Photomasks: A continuum model.

Vivek Kapila^a, Pierre A. Deymier^a, Hrishikesh Shende^a, Viraj Pandit^b, Srinu Raghavan^a and Florence O. Eschbach^c

^aDepartment of Materials Science & Engineering, University of Arizona, Tucson, AZ 85721;

^bDepartment of Electrical & Computer Engineering, University of Arizona, Tucson, AZ 85721;

^cIntel Corporation, California Technology & Manufacturing Group, Santa Clara, CA 95054

ABSTRACT

Removal of nano-scale contaminant particles from the photomasks is of critical importance to the implementation of EUV lithography for 32nm node. Megasonic cleaning has traditionally been used for photomask cleaning and extensions to sub 50nm particulates removal is being considered as a pattern damage free cleaning approach. Several mechanisms for removal are believed to be active in megasonic cleaning systems, e.g., cavitation, and acoustic streaming (Eckart, Schlichting, and microstreaming). It is often difficult to separate the effects of these individual mechanisms on contamination removal in a conventional experimental setup. Therefore, a theoretical approach is undertaken in this work with a focus on determining the contribution of acoustic streaming in cleaning process. A continuum model is used to describe the interaction between megasonic waves and a substrate (fused silica) immersed in a fluid (water). The model accounts for the viscous nature of the fluid. We calculate the acoustic vibrational modes of the system. These in turn are used to determine the acoustic streaming forces that lead to Schlichting streaming in a narrow acoustic boundary layer at the substrate/fluid interface. These forces are subsequently used to estimate the streaming velocities that may in turn apply a pressure and drag force on the contaminant particles adhering to the substrate. These effects are calculated as a function of angle of incidence, frequency and intensity of the megasonic wave. The relevance of this study is then discussed in the context of the cleaning efficiency and pattern damage in competing megasonic cleaning technologies, such as immersion, and nozzle-based systems.

Keywords: EUV lithography, Megasonic Cleaning, Acoustic Streaming.

1. INTRODUCTION

Development work on *extreme ultraviolet lithography* (EUVL) is gaining momentum as the current lithographic techniques are reaching their limits. Smaller wavelength sources are needed to produce feature sizes below 50-nm. The 13.4-nm EUVL technique is envisaged to become the method of choice for the 32-nm node by the year 2009. As the light at this wavelength is absorbed by most materials and even air, the conventional transmissive photomasks are of little use for EUVL. Instead, a composite structure formed by alternate layer of silica and molybdenum is used as photomask that reflects the EUV light.¹ A lot of effort has already been spent on developing a reflective, defect free mask structure in a collaborative effort between several industries and US national laboratories. One of the outstanding challenges in the implementation of EUVL technology is the cleaning of photomasks to remove contaminant particles of sub-50 nm sizes. The cleaning method is expected not only to be efficient in particle removal, but also the one that does not sacrifice the integrity of the patterned features.

Megasonic cleaning has been used traditionally in post-CMP cleaning of wafers as a damage free approach for the removal of sub-micron contaminant particles. In megasonic cleaning, the cassette of wafers to be cleaned is immersed in a cleaning tank with a piezoelectric transducer at the bottom of the tank. The transducer sends sound waves of 600 KHz-1 MHz frequency in the cleaning bath.² The sound waves propagating in a medium

Further author information: (Send correspondence to V. Kapila)

V. Kapila.: E-mail: vkapila@email.arizona.edu, Telephone: 1 520 626 8997

can often be represented in terms of pressure waves.³ These traveling pressure waves result in several physical effects in the liquid medium, such as cavitation, and acoustic streaming which are considered to be instrumental in the removal of contaminant particles.

Cavitation is caused by the pressure variations traveling through the liquid.⁴ The low pressure component of the sound wave causes a hole or cavity in the liquid. The cavity implodes when it can no longer support the compressive stress due to the high pressure component of the sound wave. The cavity implosion results in the transfer of energy stored in the cavity to the surroundings. This event has the potential to dislodge the contaminant particles and to even cause some damage to the substrate and the patterned features. This latter disturbing feature of cavitation is more prevalent in the ultrasonic cleaning systems employing low sound frequencies. The megasonic frequencies appear to mitigate the problem of damage, however, a clear understanding of the reasons for the same is still lacking. While some have claimed that the time between the megasonic pulses (on the order of 1.25 micro second) is too short for the formation of cavities,⁵ others have detected cavities in the megasonic tank by sonoluminescence.⁶

As the name suggests, acoustic streaming is a (time-independent) fluid motion caused by the sound wave traveling through the liquid medium. The sound wave propagating through a viscous fluid suffers attenuation resulting in a loss of acoustic momentum which is reflected in a time-independent motion of the fluid.⁷ There are several types of acoustic streaming classified in terms of scale, namely Eckart's quartz-wind like streaming,⁸ Schlichting streaming,⁹ and microstreaming.¹⁰ The boundary conditions imposed on the sound wave at the solid/viscous-fluid interface result in a fluid motion within a viscous boundary layer. This viscous boundary layer is termed *acoustic boundary layer* and depending on the frequency of the acoustic wave it can be a few microns thick. The fluid motion within the acoustic boundary layer is known as Schlichting streaming. The fluid motion caused by the attenuation of sound field outside the acoustic boundary layer is termed as Eckart's streaming. Microstreaming is a consequence of fluid vortices resulting from the scattering of sound waves from oscillating bubbles in a viscous medium.

It is apparent at this stage that any experimental investigations for the feasibility of megasonic cleaning of EUV photomasks will be clouded by the overlap of the above discussed mechanisms. Furthermore, the small spatial scales associated with the cavitation and acoustic streaming will cause difficulties in separating the effects of individual mechanisms on cleaning efficiency. Also, it will be difficult to determine the potential causes of damage to the substrate and features. Therefore, we elect to undertake a theoretical investigation of the subject. In the present work, we focus on the effects of acoustic streaming in megasonic cleaning. As we are interested in the removal of sub-50 nm contaminant particles, the Eckart's streaming operating outside the micron-thick acoustic boundary layer is expected to play little role in cleaning. Therefore, we specifically focus our attention on the effects of Schlichting streaming on the particle removal.

The article is organized as follows, the models and methods used in this work are briefly introduced in section II. Section III presents results of the calculation of the acoustic streaming force, and acoustic streaming velocity near the solid-liquid interface. Next, the streaming velocity is used to calculate the resulting drag force and rolling moments on a spherical particle adhered to a solid substrate. These are compared with the adhesion force (van der Waals) and the resistive moments on the particle. Finally, we summarize the findings of the work in section IV.

2. MODEL AND METHODS

In a previous work, Deymier et al¹¹ have obtained the streaming forces and velocities generated in megasonic systems during the cleaning of silicon wafers. As the present problem of interest, removal of nanoparticles from the EUV photomasks, is principally similar to the previously reported work, we follow the model of Deymier.¹¹ Here we only briefly recall the main features of their model and methods and make use of the appropriate equations developed there without re-deriving them.

In a typical megasonic cleaning system, the disc-shaped substrates (wafer or photomask) to be cleaned are immersed in a cleaning tank filled with an aqueous solution. Such a system can then be modeled as a layered composite, one with alternate layers of fluid and solid substrate, as shown in Fig. 1. Since the diameter of the

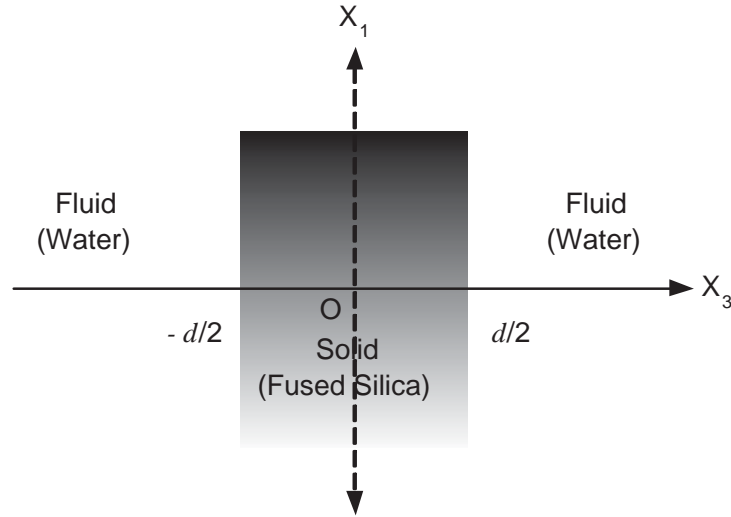


Figure 1. Illustration of the fluid/solid/fluid model.

substrate is much larger than its thickness, the layered composite can be treated as being infinite in directions parallel to the solid/fluid interface. Also, for the sake of simplicity the solid medium is considered to be isotropic.

The acoustic streaming due to a sound wave propagating through a viscous medium is known to be a viscosity induced second order effect. Often, acoustic streaming is treated as the nonlinear correction to the linear (first order) acoustic field in a viscous medium. Therefore, we first calculate a first order (time-dependent) acoustic displacement field at a solid/viscous-fluid interface and then use it to obtain the time-independent (second-order) pressure field. We make use of the interface response theory (IRT)¹² based on a Green's function formalism to obtain the first-order acoustic displacement field. Next, an approach developed by Nyborg¹³ is used to obtain the acoustic streaming force and acoustic streaming velocity from the first-order acoustic displacement field. The equations developed in¹¹ provide streaming forces and streaming velocities normalized to the amplitude (B) of the incident wave. Since, in practice, power (or intensity) of the megasonic wave is used as a controllable parameter, we normalize the streaming forces and velocities with respect to the intensity of the wave using³

$$B = \frac{1}{2\pi f} \sqrt{\frac{2I}{\rho_0 c_0}}, \quad (1)$$

where f is the frequency and I is the intensity of the megasonic wave, ρ_0 is the density of water and c_0 is the speed of sound in water.

3. RESULTS

The recent industrial activity in the megasonic cleaning is focused on using 3 MHz frequency in order to minimize cavitation in the cleaning tank. Therefore, in this work we use acoustic waves with a frequency of 3 MHz to simulate the effect of acoustic streaming in particle removal. The solid substrate modeled in this work is considered to be made of fused silica with a thickness of 6.35 mm. The input parameters used in the calculations of streaming forces and velocities are: a density of $2.2 \times 10^3 \text{ Kg/m}^3$, a Young's modulus of 72.6 MPa, and a Poisson's ratio of 0.16 for fused silica, and a density of 10^3 Kg/m^3 and a viscosity of 10^{-3} Pa-s for water. The longitudinal speed of sound in water is taken to be 1500 m/s. The longitudinal and transverse speeds of sound in fused silica are calculated to be 5929 m/s and 3771.3 m/s, respectively.

Following Deymier,¹¹ we first calculate the streaming force as a function of the wave vector $k_{||}$ of the incident megasonic wave at a distance of $0.1 \mu\text{m}$ from the substrate (Fig. 2). The peaks in this curve correspond to the

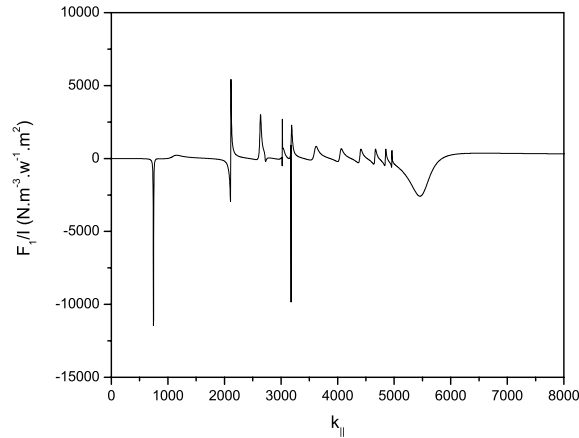


Figure 2. Streaming force as a function of the wave vector $k_{||}$ of the incident megasonic wave.

acoustic modes of vibration excited by the megasonic wave of frequency 3 MHz. The large peak at $k_{||} = 3175.49 \text{ m}^{-1}$ suggests that streaming force F_1 is sufficiently strong here to warrant further examination. We, therefore, calculate the streaming force for waves with $k_{||} = 3175.49 \text{ m}^{-1}$ as a function of distance from the substrate. In our calculations we find that the component of streaming force normal to the fluid/substrate interface (F_3) is much smaller than the one parallel to the interface (F_1), i.e., $F_3 \ll F_1$. Therefore, only the force profile corresponding to F_1 is presented in Fig. 3. The streaming velocity is then calculated using an equation derived by Nyborg

$$\mu \Delta^2 \mathbf{v}_2 = \Delta p_2 - \mathbf{F}, \quad (2)$$

where μ is the viscosity of the fluid, \mathbf{v}_2 is the streaming velocity, and \mathbf{F} is the streaming force. Assuming $F_3 = 0$ since $F_3 \ll F_1$) leads to the following simplified form of (2)

$$\frac{\partial^2 v_1}{\partial X_3^2} = -\frac{F_1}{\mu} = D(X_3) \quad (3)$$

The solution of Eq. 3 is then given by¹³

$$v_1(X_3) = X_3 \left[-\int_0^\infty D(\alpha) d\alpha + \int_0^{X_3} D(\alpha) d\alpha \right] - \alpha \int_0^{X_3} \alpha D(\alpha) d\alpha \quad (4)$$

Eq. 4 is then solved numerically to calculate the streaming velocity as a function of distance from the substrate (Fig. 4). Since streaming force and velocity vary only in a thin region of thickness of $\sim 1.5 \mu\text{m}$ (Figs. (3) and (4)), the acoustic boundary layer thickness is estimated to be $1.5 \mu\text{m}$.

The forces acting on a particle adhered to a solid substrate and subjected to megasonic cleaning are represented in Fig. 5.¹⁴ Here, F_D represents the drag force on the particle due to fluid motion, F_L represents the lift force on the particle due to pressure differential in the fluid normal to the fluid/solid interface, F_A is the adhesion force between particle and the substrate, and M_D is the hydrodynamic moment.

The adhesion force on the particle is calculated as the van der Waals force of adhesion between a spherical particle and a planar surface

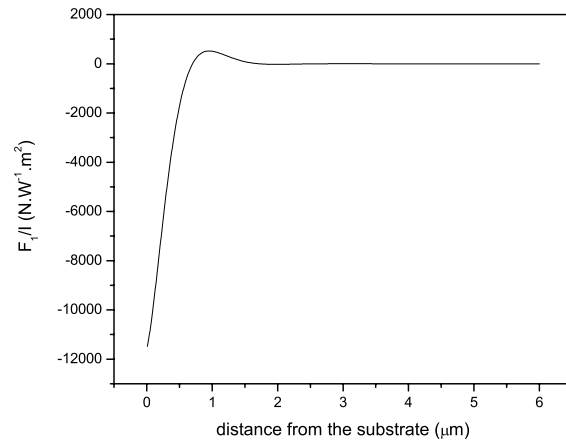


Figure 3. Streaming force as a function of distance from the substrate for $k_{||} = 3175.49 \text{ m}^{-1}$.

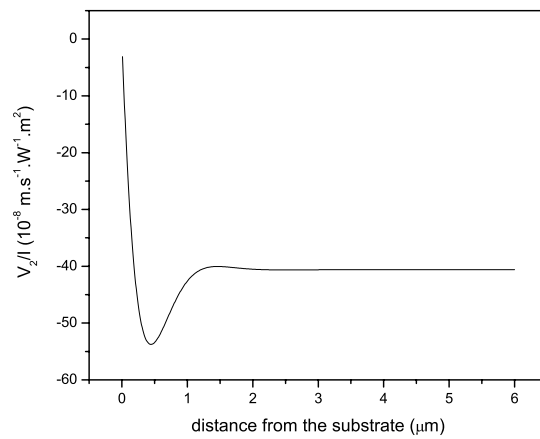


Figure 4. Streaming velocity as a function of distance from the substrate.

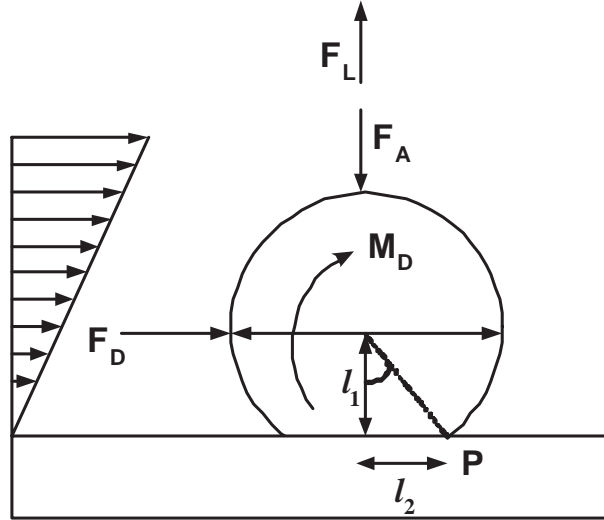


Figure 5. Forces and moments on a spherical particle in a linear fluid flow.

$$F_A = \frac{A_{132}r_0}{6(X_3 - r_0)^2}, \quad (5)$$

where X_3 is the distance between the center of the particle and the surface, A_{132} is the effective Hamaker constant and is taken to be as $A_{132} = 0.83 \times 10^{-20} \text{J}^{11}$ for a silica particle adhered to a silica surface in an aqueous medium. The quantity $(X_3 - r_0)$ is defined as the distance (h) between particle and the substrate. When the particle is in near contact with the surface, a deformation of the particle, or of the surface, or of both can occur. This deformation increases the interaction area between the surface and the particle. The van der Waals force then gets modified as

$$F_A = \frac{A_{132}r_0}{6h^2} \left(1 + \frac{a^2}{hr_0} \right), \quad (6)$$

where a is the contact radius between particle and the surface and depends on the properties of the materials involved. In our calculations of adhesion force we have neglected the effect of deformation. However, we discuss the possible impact of this deformation on our results while comparing the adhesion force with the removal forces.

As long as the flow of fluid over the particle diameter is linear (as shown in Fig. 5), the drag force and the hydrodynamic moment on the particle can be calculated as¹⁵

$$F_D = 1.7009 \cdot (3\pi\mu dV_p), \quad (7)$$

and

$$M_D = 0.9439934 \cdot (2\pi\mu d^2V_p), \quad (8)$$

where V_p is the fluid velocity at the center of the spherical particle.

The conditions to be satisfied for the particle removal are given by¹⁴

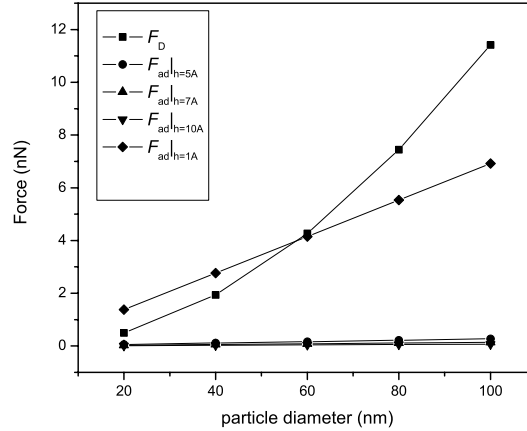


Figure 6. Drag and adhesion forces on the particles as a function of particle size.

$$\begin{aligned}
 F_D &\geq C_f(F_A + F_L) && \text{Sliding mechanism,} \\
 M_D + F_D l_1 + F_L l_2 &\geq F_A l_2 && \text{Rolling mechanism,}
 \end{aligned} \tag{9}$$

where C_f is the friction coefficient between particle and substrate, and l_1 and l_2 are the lever arms for F_D , and F_A and F_L , respectively. Typically, the lift force in the megasonic system is considerably smaller compared to F_d , and F_A . It is then possible to neglect the effect of lift force in the Eqns. (9) leading to following simplified form

$$\begin{aligned}
 F_D &\geq C_f F_A && \text{Sliding mechanism,} \\
 M_D + F_D l_1 &\geq F_A l_2 && \text{Rolling mechanism,}
 \end{aligned} \tag{10}$$

We consider here the removal of particles with diameter $d \leq 100$ nm. As can be seen from Fig. 4, the velocity profile is linear in this range, permitting the use of equations (7) and (8). In calculating the drag forces and moments using the streaming velocities in Fig. 4, we use an intensity of 5×10^7 W/m² for the megasonic wave. This intensity corresponds to an input power of 50 W with the transducer area of 0.01 cm². Although the intensity used here may be an overestimate of the intensities used in an immersion type megasonic system, it is well within the range of the intensities used in the nozzle-based megasonic systems. In Fig. 6 we show the drag force on the particles in the size range $d \in [20, 100]$ nm and compare it with the adhesion force on the particles for several separation distances from the substrate. It is seen that the drag force is much higher in comparison to the adhesion forces at $h = 5, 7,$ and 10 \AA . Additionally, the adhesion force is seen to be larger than the drag force for $h = 1 \text{ \AA}$ for particles with $d < 60$ nm. However, it must be noted here that the distance $h = 1 \text{ \AA}$ provides only an upper bound on the adhesion force. In real systems, the separation distance between the particle and substrate is considered to be $\sim 4 \text{ \AA}$.¹⁴ At this distance, the drag force is again expected to be much larger than the adhesion force. Also, since the drag force on the particle is proportional to the streaming velocity (normalized to the intensity), an order of magnitude smaller intensity will result in an order of magnitude smaller drag force. As can be seen in Fig. 6 the drag force still remains larger than the adhesion force at $h = 5, 7,$ and 10 \AA .

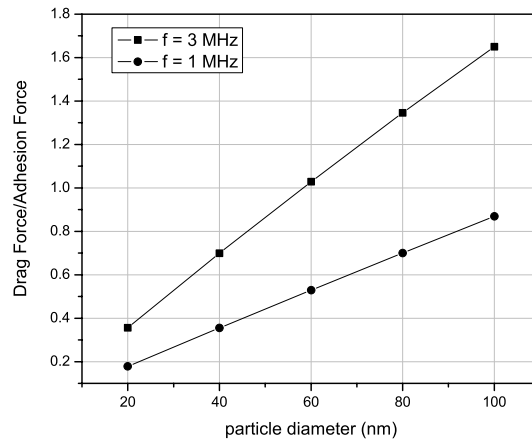


Figure 7. Ratio F_D/F_A at $h = 1 \text{ \AA}$ as a function of particle diameter; $k_{||} = 3149.75 \text{ m}^{-1}$ for $f = 3 \text{ MHz}$, and $k_{||} = 2160.16 \text{ m}^{-1}$ for $f = 1 \text{ MHz}$.

Next, considering that the drag and adhesion forces are normal to each other, a direct comparison of the two is of little interest from the particle removal point of view. Instead, the ratio of the drag force and adhesion force is of a more fundamental importance as is indicated by Eq. 10. According to Eq. 10, the condition for particle removal is satisfied as long as the ratio F_D/F_A is greater than the coefficient of friction, C_f , between particle and the substrate. The friction coefficient for any two bodies in sliding contact is always between 0 and 1 ($C_f \in [0, 1]$). According to Fig. 6, the ratio F_D/F_A is always larger than 1 at separation distances of $h = 5, 7$, and 10 \AA indicating removal of all particle sizes. Next, we plot the ratio F_D/F_A as a function of particle diameter for $h = 1 \text{ \AA}$ (Fig. 7). It is seen from this figure that as long as the friction coefficient between particle and the substrate is less than 0.4, all the particles with diameter $d \geq 20 \text{ nm}$ can be removed by sliding mechanism. Although, the true friction coefficient between the particle and the substrate is not known, a recent molecular dynamics study¹⁶ of friction between two alkylsilane monolayer coated silica substrates calculated a friction coefficient of 0.1-0.3. Therefore, a reasonable first guess for the friction coefficient between particle and substrate can be considered to be ~ 0.3 . Even when $\mu = 1.0$ (worst case!), Fig. 7 indicates that megasonic cleaning at 3 MHz can potentially remove all particles down to sizes $\sim 60 \text{ nm}$ with sliding mechanism. For comparison purposes, we have also calculated drag force on particles due to the acoustic streaming resulting from megasonic waves of frequency $f = 1 \text{ MHz}$. The ratio F_D/F_A for this frequency (and $k_{||} = 2160.16 \text{ m}^{-1}$) is also plotted in Fig. 7. It is seen from Fig. 7 that at $f = 1 \text{ MHz}$, the removal of particles with $d < 60 \text{ nm}$ requires $C_f < 0.55$. In other words, removal of smaller particles at $f = 1 \text{ MHz}$ will require much smoother surfaces than in the case of megasonic waves with $f = 3 \text{ MHz}$.

As mentioned before, we have neglected the effect of particle deformation in the calculation of the adhesion force F_A . In Eq. 6, we can express a and h as multiples of r_0 , i.e., $a = m \cdot r_0$, and $h = n \cdot r_0$. The effect of deformation on adhesion force increases with increasing m and decreasing n . Assuming a fix value of $h = 0.4 \text{ \AA}$, n is smallest for $r_0 = 50 \text{ nm}$. Next, assuming a deformation of particle corresponding to $n = 1/5$ (significant deformation!), the correction term is calculated to be equal to 5. This indicates that the adhesion force calculated without incorporating the effect of deformation is less than an order of magnitude smaller. According to Fig. 6, the drag force will still be larger than the adhesion force at $h = 5, 7$, and 10 \AA for a large range of particle sizes.

A particle in near contact with the surface can also lead to the deformation of either the particle, the surface or both. Such deformation can provide a point (P in Fig. 5) about which the hydrodynamic moment M_D and the moment of drag force F_D can apply a torque to set the particle in a rolling motion. Similarly, the point P could also be a point of contact between the particle and an asperity on a rough surface. The rolling motion is

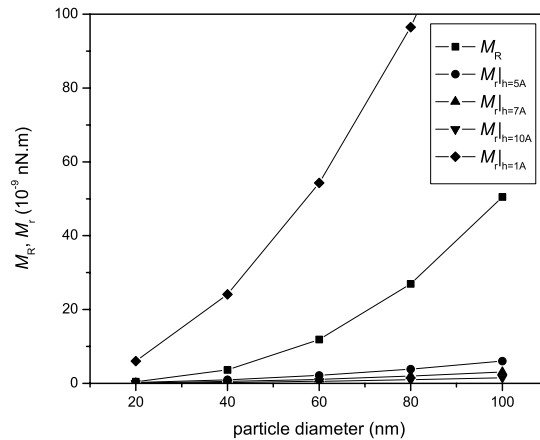


Figure 8. Removal(M_R) and resistive (M_r) moments on the particles as a function of particle size.

resisted by the moment of adhesion force acting in the opposite direction. The conditions for removal by rolling mechanism are then set forth by Eq. 10. We refer to the left side of the moment equation in Eq. 10 as removal moment (M_R), and the right side as resistive moment (M_r). The relative amounts of the removal moment and the resistive moments will also depend on the length of the lever arms l_1 , and l_2 . As the point P moves away from the center of the particle, in a direction parallel to the substrate (larger deformation or surface roughness), the length of lever arm l_1 decreases and length of lever arm l_2 increases. As a first estimate, the lever arms l_1 , and l_2 can be related as

$$l_2 = l_1 \sin \theta, \quad (11)$$

where θ is the angle between lever arm l_1 and the line connecting the center of particle and the point P. We compare the removal and resistive moments as a function of particle size in Fig. 8 for $l_1 = 0.45d$. It is seen from Fig. 8 that the removal moment is appreciably larger than the resistive moments for separation distances of $h = 5, 7$, and 10 \AA for all particle sizes. However, the removal moment fails to overcome the resistive moment at $h = 1 \text{ \AA}$. Again, the separation distance of 1 \AA is only an upper bound in the calculation of adhesion forces and the resistive moment. Considering a realistic separation of $\sim 4 \text{ \AA}$, Fig. 8 suggests that the resistive moment curve for $h = 4 \text{ \AA}$ will lie between the curves for M_r at $h = 5 \text{ \AA}$ and M_R . This indicates that rolling mechanism can also remove most particle sizes at the megasonic frequency of 3 MHz. Also, the effect of deformation induced modification of adhesion force on the resistive moment can be explained in the same way as in the discussion of removal by sliding mechanism.

4. CONCLUSIONS

A continuum model study has been performed to investigate the feasibility of megasonic cleaning method for removing sub-50 nm particles adhered to the photomask material. In particular, we study the effect of acoustic streaming in particle removal. The current work is of fundamental importance to the implementation of EUVL technology for the generation of 32-nm node in chip manufacturing. We use the methods based on interface response theory and a method due to Nyborg to calculate acoustic streaming forces and velocities in the vicinity of the solid/viscous-fluid interface. These in turn are used to calculate the drag forces and rolling moments on a spherical particle adhered to a fused-silica substrate. We consider a van der Waals adhesion force between the particle and the surface. Although not specifically calculated, the effect of deformation of surfaces on the adhesion

force is also discussed. The calculations show that the Schlichting streaming velocity in a thin acoustic boundary layer due to the megasonic waves can give rise to sufficiently strong drag forces and rolling moments to remove the adhered particles via sliding and rolling mechanisms. A comparison of particle removal with sliding mechanism at two different megasonic frequencies of 1 MHz, and 3 MHz shows that cleaning at lower frequencies would require much smoother surfaces of particle and substrate. This suggests that for the removal of small particles ($d < 60$ nm), megasonic frequencies of 3 MHz would be more appropriate. Future work will include experimental validation of simulation results on photomask blanks. Removal of particulates using Megasonics clean process without inducing damage to sub 90nm node patterned photomask features remains a challenge. Future modeling work will focus on evaluating microcavitation effects on integrity of patterned photomask minimal feature size and substrate to assess Megasonics induced damage.

REFERENCES

1. G. Stix, "Getting more from moore's," *Scientific American* **284**, p. 32, 2001.
2. A. A. Busnaina, I. I. Kashkoush, and G. W. Gale, "An experimental-study of megasonic cleaning of silicon-wafers," *J. Electrochem. Soc.* **142**, p. 2812, 1995.
3. R. Resnick and D. Halliday, *Physics*, Wiley, NewYork, 1990.
4. F. R. Young, *Cavitation*, McGraw-Hill, London, 1989.
5. S. Schwatzman, A. Mayer, and W. Kern *RCA Rev.* **46**, p. 81, 1985.
6. R. Gouk, "Experimental study of acoustic pressure and cavitation field in a megasonic tank," Master's thesis, University of Minnesota, 1996.
7. D. Zhang, *Fundamental study of megasonic cleaning*. PhD thesis, University of Minnesota, 1993.
8. C. Eckart, "Vortices and streams caused by sound waves," *Phys. Rev.* **73**, pp. 68–76, 1948.
9. H. Schlichting, *Boundary-Layer Theory*, McGraw-Hill, NewYork, 1968.
10. S. Elder, "Cavitation microstreaming," *J. Acoust. Soc. Am.* **31**, p. 54, 1959.
11. P. A. Deymier, J. O. Vasseur, A. Khelif, B. Djafari-Rouhani, L. Dobrzynski, and S. Raghavan, "Streaming and removal forces due to second-order sound field during megasonic cleaning of silicon wafers," *J. Appl. Phys.* **88**, pp. 6821–6835, 2000.
12. L. Dobrzynski, "Interface response theory of continuous composite materials," *Surf. Sci.* **180**, pp. 489–504, 1987.
13. W. L. Nyborg, "Acoustic streaming," in *Physical Acoustics - Vol. II B*, W. P. Mason, ed., pp. 265–331, Academic, London, 1965.
14. G. M. Burdick, N. S. Berman, and S. P. Beaudoin, "Describing hydrodynamic particle removal from surfaces using the particle reynold's number," *J. Nanoparticle Research* **3**, pp. 455–467, 2001.
15. M. O'Neill, "A sphere in contact with a plane wall in a slow linear shear flow," *Chem. Eng. Sci.* **23**, p. 1293, 1968.
16. V. Kapila, *Molecular simulations of surfactants and silanes: self-assembly in solutions and on surfaces and friction between monolayers*. PhD thesis, University of Arizona, 2004.